Journal of Visualization, Vol. 9, No. 2 (2006)179-187

A Study of Premixed Propagating Flame Vortex Interaction

Hargrave, G. K.* and Jarvis, S.*

* Wolfson School of Mechanical and Manufacturing Engineering, Loughborough University, Loughborough, Leicestershire, LE11 3TU, UK. Tel: +44(0)1509 227526/FAX: +44(0)1509 227704, E-mail: g.k.Hargrave@lboro.ac.uk

Received 24 March 2005
Revised 29 July 2005

Abstract : Experimental data is presented for the interaction between a propagating flame and a simple vortex flow field structure generated in the wake of solid obstacles. The interaction between gas movement and obstacles creates vortex shedding forming a simple flow field recirculation. The presence of the simple turbulent structure within the gas mixture curls the flame front increasing curvature and enhancing burning rate. A novel twin camera Particle Image Velocimetry, PIV, was employed to characterise the flow field recirculation and the interaction with the flame front. The technique allowed the quantification of the flame/vortex interaction. The twin camera technique provides data to define the spatial variation of both the velocity of the flow field and flame front. Experimentally obtained values of local flame displacement speed and flame stretch rate are presented for simple flame/vortex interactions.

Keywords : Combustion, Flame/Vortex, PIV, Visualization.

1. Introduction

In order to improve our understanding of some of the fundamental aspects that form the complex phenomenon that is turbulent premixed combustion, studies of simple idealized vortex/flame interactions are required. For studies on turbulent combustion a recognised method of generating a simplistic situation is to allow a propagating laminar flame to interact with a single vortex structure. Examples of such investigation have been completed by Eichenberger and Roberts (1999), Mueller et al. (1996), and Lee et al. (1993). Thus, this paper presents high quality laser diagnostic results taken from a series of investigations on flame/vortex interactions within a small scale combustion chamber.

Numerous studies presented in literature have investigated laminar flames interacting with vortices based on the knowledge that many practical turbulent combustion systems operate in the wrinkled laminar flame region of the combustion diagram. Combustion diagrams, such as that presented by Borghi (1985) provide a basis of quantifying combustion regimes in terms of dimensionless parameters such as the turbulent Damkohler number, Reynolds number and Karlovitz number. Poinsot et al. (1991, 1996) completed a numerical study into the effect of flame/vortex interactions on basic flame front characteristics. The study predicted that classical combustion regime diagrams under-estimated the resistance of flame fronts to turbulent eddies. Experimental studies utilising laser tomography and PLIF were presented by Roberts et al. (1991, 1993) into the effect of flame/vortex interactions. The work provided observations on the vortex disturbance of the flame front, and quantification of the vortex quenching limit. Further experimental studies conducted by Mueller et al. (1995, 1996) using both PIV and LIF investigated

the effect of local stretch rate on the flame chemistry. It was found that heat losses, and positive and negative curvature had a marked effect on the flame chemistry, eventually leading to extinction. Samaniego and Mantel (1999) presented an alternative study providing data on a rod-stabilised flame interacting with propagating slot-generated vortices. Samaniego and Mantel (1999) observed that the flame/vortex interaction take places in the quenching regime proposed by Poinsot et al. (1991), however no quenching occurred.

Continued studies on the flame/vortex interaction phenomena completed by Sinibaldi et al. (1998) concentrated on quantification of the local flame displacement speed and flame stretch rate. High speed recordings of flame front position and local flow velocity were completed using a tomography and PIV technique. Data for flame velocity, V_f, and flow field velocity, V_r, in a direction normal to the flame surface was then combined to calculate local flame displacement speed, S_d

$$S_d = V_f \cdot \overline{n} - V_r \cdot \overline{n} \tag{1}$$

where $\overline{n}$ is the unit normal to the thin flame segment. The total flame stretch, K, was also proposed as the sum of the strain component K_S and the curvature component K_C, such that $K = K_S + K_C$. Results showed only positive values of S_d were obtained varying up to five times that of the unstretched laminar flame speed. A similar technique was employed by Ibarreta and Driscoll (2000) to investigate the effect of negative curvature during flame/vortex interactions. The results provided a correlation between burning velocity and curvature for inwardly propagating flames.

Examples presented in literature show that the majority of previous work completed on flame/vortex interactions concentrated on a vortex pair generated as a result of a pulse jet. Formation of the vortex pair occurred as the flammable working fluid was driven through a sharp edged orifice (Louch and Bray, 2001). An example of this configuration was that utilised by Roberts et al. (1991, 1993) and Mueller et al. (1995), in which a square cross section combustion chamber was employed that consisted of an upper and lower chamber. The lower chamber contained the standard spark ignition system, and was separated from the upper chamber by an interchangeable sharp edged orifice plate. The upper chamber was sealed using a loud speaker. Mixture contained within the two chambers was ignited which resulted in a laminar flame propagating upwards, and interacting with a toroidal vortex pair that was generated by fluid forced through the orifice by movement of the speaker cone. Modifications to the design were introduced by Mueller et al. (1996, 1998), which involved inverting the combustion chamber.

In view of the previous studies on flame/vortex interactions it was chosen to employ a square cross section combustion chamber incorporating a fluid pulse vortex formation technique. However, differing from literature, a more practical simplistic approach was employed utilising a pair of obstacles positioned downstream of the ignition point. Thus, the work presented in this paper details the application of both standard PIV and a novel twin camera PIV technique to provide visualization and quantification of flame/vortex interactions within the practical geometry. The authors were able to provide the accurate measurement of both flame position and local flow field velocity to allow the calculation of the flame displacement speed, and flame stretch rate based on theory presented previously in literature.

2. Experimental Configuration

2.1 Combustion Chamber

The development of the combustion chamber was based on the generation of simple single vortex turbulent structures, into which a laminar flame front could propagate. A schematic of the combustion chamber, shown in Fig. 1, highlights the geometry and location of the obstacles in

relation to the ignition source. The design was based on the theory that gas contained within the chamber would be forced through the gap located between the two obstacles, resulting in the formation of a vortex pair. Part of the ignited flame would then follow the same path as the vortex forming mixture, jetting through the opening and interacting with the vortices. The combustion chamber was manufactured from clear polycarbonate to aid optical access and provided a 150 mm by 150 mm internal cross section. The chamber was 150 mm in height, closed at the lower end and open at the opposite end to allow the flame to vent. A pair of 10 mm thick aluminum obstacles where located at a height of 75 mm above the base plate together with a 50 % blockage on the chamber exit. For data presented in this paper a 5 mm spacing between obstacles was employed. Each obstacle was fixed in place and ran from the front face of the chamber, to the rear.

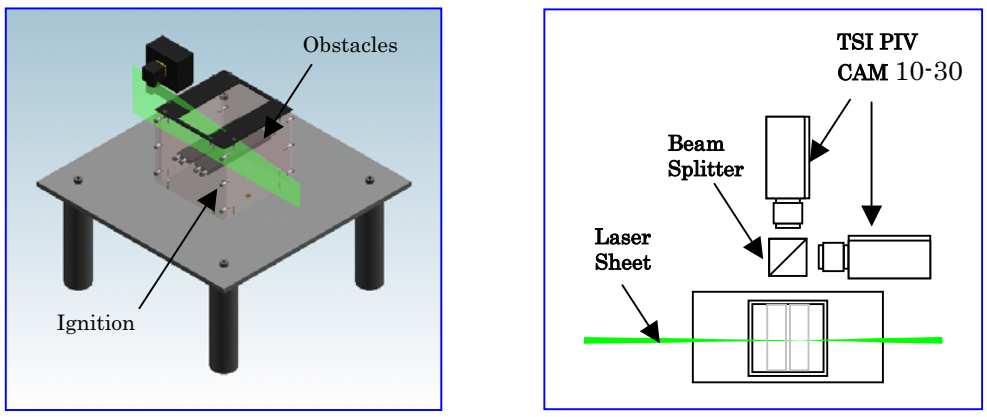

Fig. 1. The combustion chamber for the study of flame/vortex interactions and laser diagnostic setup.

For the purpose of this study a premixed mixture of methane and air was generated within the combustion chamber. A stoichiometric mixture, $\phi = 1.0$, was provided with the mixture purged thorough the combustion chamber for 150 s to ensure homogeneity, and then left to settle for a further 30 s prior to ignition to ensure dissipation of all flow structures generated during the mixing process. Containment of the flammable charge was achieved by placing a thin plastic membrane on the chamber exit, which ruptured on ignition of the flame. Initiation of the flammable mixture was achieved using a standard automotive spark system synchronized with the triggering of the laser diagnostics.

2.2 Laser Diagnostics

For detailed characterisation and quantification of the flame/vortex interaction a novel twin camera digital PIV (DPIV) technique was employed. The measurement setup consisted of two independent DPIV systems monitoring exactly the same region within the combustion chamber. Figure 1 presents

a schematic of the system highlighting the combination of each independent setup, positional alignment of laser sheets and the use of a beam splitter for accurate capture of the same area of interest. For each independent setup the light emitted from a double pulse Nd;YAG laser (532 nm) was formed into a vertical sheet and introduced into the combustion chamber to provide an illumination plane 70 mm high by 1 mm wide. The 1000 by 1016 pixel resolution cameras were mounted an equal distance from a beam splitter and set to image a region approximately 30 mm by 30 mm above the top surface of the obstacle on the chamber centerline. Light scattered from olive oil flow tracing material of approximate diameter 1-2 μm was imaged through 50 mm AF Micro Nikkor lenses providing an averaged imaged particle size covering 1.44 pixels. Each PIV system was operated in the standard 15 Hz two frame capture mode, with a pulse separation of 10 μs. In order to capture the temporal development of the flame front the twin camera PIV setup was employed. The separation of each DPIV system was achieved using polorisation control. This allowed a variable time separation between captured velocity fields of 50 μs to 300 μs. Thus providing temporal development of the flame/vortex interaction at one instance during the flame front propagation. For the purpose of the work presented in this paper a time separation of 300 μs was utilised.

Image pairs were analysed using a two frame cross correlation routine incorporating a Guassian peak search algorithm within a commercially available package. For the data presented in this paper an interrogation region of 32 by 32 pixels with a 50 % positional overlap was employed which equated to a 0.978 mm by 0.978 mm interrogation region size.

3. Results and Discussion

Preliminary investigations completed by the current authors concentrated on varying both obstacle geometry and exit blockage to control the vortex structures generated. Results from the investigation into the combustion chamber geometry highlighted the nature of the vortex flow structures and flame front geometries generated with a 5 mm obstacle gap. Stability of the vortex structures and the regularity of development was apparent. Figure 2 presents a typical sequence to highlight the flow and flame front development within the combustion chamber. High resolution digital images clearly show the development of small scale vortex structures from the inside edge of each of the obstacles. Pairs of vortices are formed from the obstacle gap, while development of the flame into the flow structures is seen over the period t = 23.2 ms to t = 26.2 ms. During the initial phase the flame propagates in free form taking a laminar flame shape. The recirculating structures ahead of the flame continue to develop. At t = 23.8 ms the flame begins to interact with the flow structures, resulting in a narrowing of the most downstream area of the flame front. Flow structures formed either side of the flame also take effect causing the lower flame edge to curl out. Throughout the second phase of the flame propagation the flame front continues to interact with flow structures located ahead and to the side. At t = 25.2 ms the lower half of the flame front has curled into flow recirculations at two positions either side of the centre line. The upper half of the flame has narrowed as it passed between the most downstream vortex pair. The final image in the sequence highlights the main body of the flame interacting with the flow structures formed as the upper most tip has propagated out of the image area

Based on the results obtained from the preliminary investigation the scale of vortex structures produced was used to characterise the regime of flame/vortex interactions observed. Comparison of flame/vortex parameters can be made based on those presented in literature taking into account the rotational speed of the vortex, U_θ, and the core diameter of the vortex, d_c. Samaniego and Mantel (1999) proposed a definition of the conditions of flame/vortex interaction, plotting a vortex flame diagram based on the dimensionless parameters U_θ/S_L versus d_C/δ_L. The diagram clearly defines areas of no effect, wrinkling and quenching. For relevance to the work of this study, data points taken from flame/vortex investigations completed by the current authors are found to occur within the wrinkling flame regime.

To further quantify the flame/vortex interactions observed DPIV measurements of the development were taken. The measured velocity field data corresponding to the image sequence shown in Fig. 2 is presented in Fig. 3. Arrows added to the figure clarify the direction and size of the recirculations formed as the vortex shedding occurs, with the flame front is highlighted by the blank area. High flow field velocities in the region ahead of the flame can be seen, together with large increase in the size and speed of recirculations downstream of the flame front. This is a direct result of the acceleration of the flame front as it passes through the obstacle gap. At time t = 23.8 ms the flow field can be seen to be effecting the flame front geometry, resulting in distortion of the flame surface. With increased time after ignition the flame front can be seen to develop further downstream and interact with the recirculation flow structures. The flame front surface is then further distorted by the flow structures.

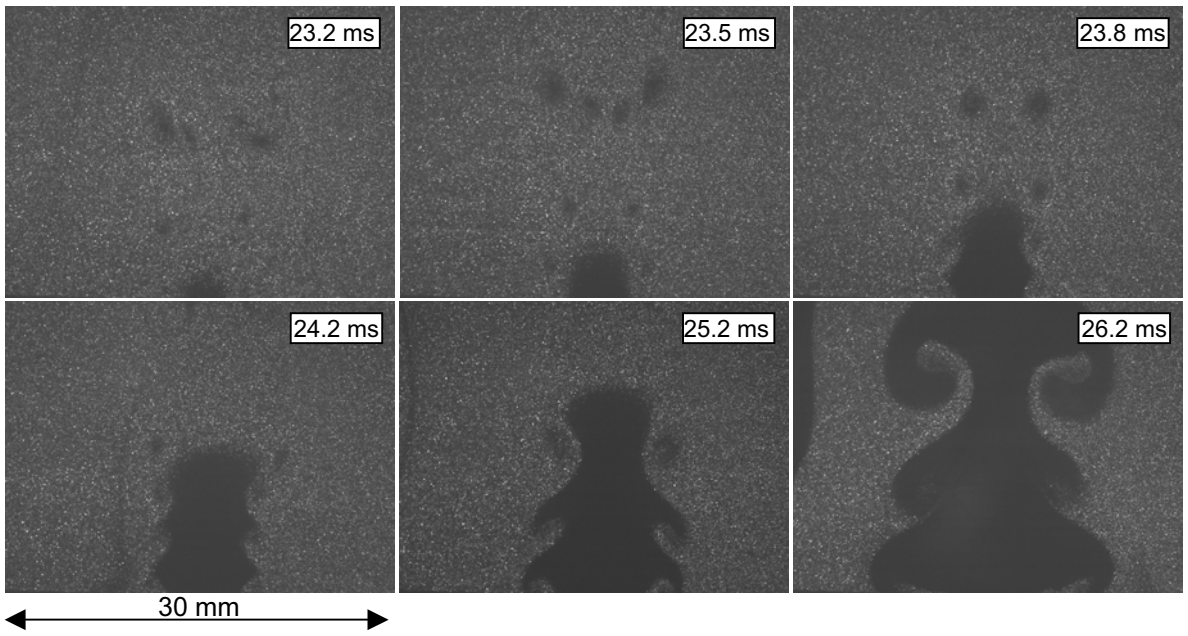

Fig. 2. High resolution digital image sequence depicting mode of flow and flame development in wake of 5 mm spaced obstacles and 50 % exit blockage.

Based on results obtained from the twin camera DPIV technique flame front locations were obtained at two instances separated by 300 μs for an example interaction case, approximately 24.5 ms after ignition. Figure 4(a) presents derived flame front position data taken from the high resolution first frame image at each instance for 70 locations around the flame surface. The data clearly highlights the overall downstream propagation of the flame front over the separation period, and the interaction with flow field recirculations in the lower regions. Interestingly lower regions of the flame front in the regions close to the flow field recirculation appear to propagate into a region previously occupied by burnt gas. This is believed to be a direct result of the interaction between flame and flow as fresh charge is convected into the previously flame occupied region. Overall the flame surface area increases highlighting the increase in burn rate as the flame interacts with the turbulent structure.

Figure 4(b) presents the calculated results for flame speed between the displaced initial flame front and the second flame front, and measured flow velocity for the example case. The results show an almost uniform flame speed along the most downstream edge of the flame front. Flame velocities around the region where the flame is interacting with the recirculation structures show differing properties. In the areas of positive curvature, the flame is convex to the flow, flame speed is directed towards the unburnt mixture, whereas areas of negative curvature show flame speed directed towards the burnt gas. Interestingly the lower left central region of the flame front shows large flame speeds in the direction of the burnt gas. Comparison of the flow velocity in this region indicates a

large variance in direction, as the flow moves in an almost vertical manner. Differences in the direction of the flow and flame can be seen round the entire perimeter of the flame surface. Significantly, the flow can be seen directed at different angles to the assumed normal motion of the flame.

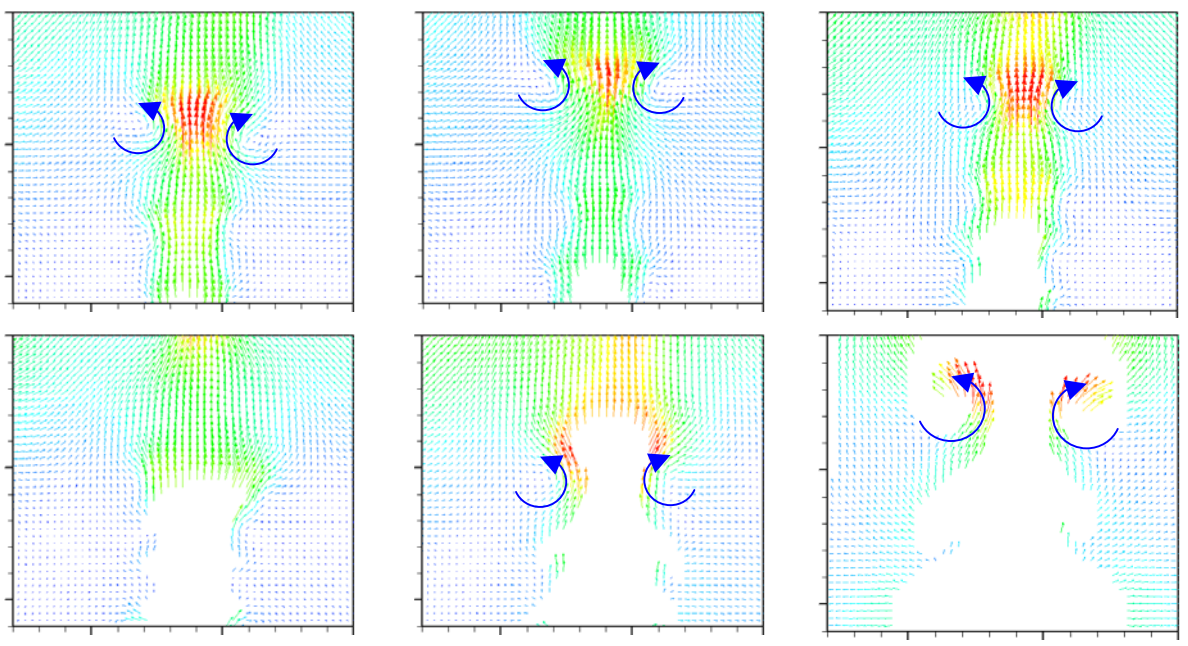

Fig. 3. Cross correlated PIV images showing flow field development in wake of 5 mm spaced obstacles and 50 % exit blockage.

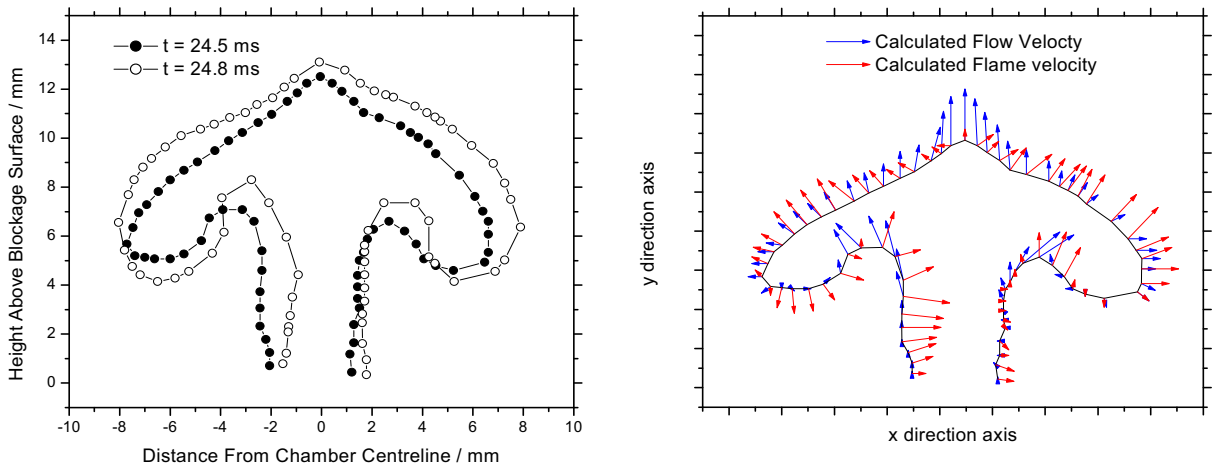

(a) (b)

Fig. 4. (a) Measured typical flame front locations in wake region of obstacles, at a time separation of 300 μs taken from twin camera DPIV investigation, (b) Twin camera PIV analysis diagram of chosen vortex flame interaction. Arrows represent measured flow and flame velocity at 70 locations around flame front.

Analysis of a propagating flame front interacting with a vortex using a similar technique to that previously described by Sinibaldi et al. (1998), allowed the calculation of a local flame displacement speed using Eq. (1). Literature also highlighted the possibility of further data extraction from the application of the twin camera DPIV technique. Capture of the flow field velocity ahead of the flame, and knowledge of the direction in which the flame front burns normal to its surface allows the calculation of the local tangential strain rate, S_{tt}. Renou et al. (1998) based on a

study of a freely propagating flame interacting with a decaying isotropic turbulent flow suggested that the S_{tt} could be determined utilising

$$S_{tt} = \frac{\partial u_t}{\partial s} \tag{2}$$

where u_t is the tangential velocity of the fresh mixture ahead of the flame, and s is the distance along the flame surface. Having calculated the tangential strain rate, Renou et al. (1998) also proposed the calculation of the local flame stretch rate, K, such that $K = S_{tt} + S_d h$ where S_d is the local flame displacement speed and h the radius of curvature.

Figure 5 presents the calculated flame displacement speed relative to the measured radius of curvature of the flame front. The figure shows values for S_d normalised with respect to the unstretched laminar flame speed, and the radius of curvature relative to the distance around the flame. Moving from the lower right hand side of the flame front the change in flame shape and so curvature are apparent. Along the initial part of the flame surface the curvature is positive, but as the region where the flame is assumed to be interacting with the vortex structure is approached the curvature becomes negative. As discussed above this is matched by an increase in calculated flame displacement speed. Continuing around the flame front the curvature becomes positive and relatively constant, this corresponds to an approximately constant displacement speed. Notably, the radius of curvature shows a sharp change, becoming negative before returning to a positive value. This matches the flame shape in the most downstream section of the flame front. As discussed previously, the tip of the flame begins to interact with downstream flow structures, narrowing, and causing a sudden change in curvature along the flame surface. Following the change in curvature, the flame displacement speed begins to decrease, and reaches a minimum at approximately 25 mm corresponding to the flame tip where the radius of curvature is positive. A similar trend to that discussed can then be seen as the rest of the flame surface is navigated. The symmetry in the flow structures and generated flame shape shows the relatively constant S_d with slowly decreasing radius. Continuing around the flame front, negative flame displacement speed is apparent in the region of negative curvature which corresponds to the section of the flame interacting with the left hand vortex.

Comparisons of values of S_d/S_L for flame-vortex interactions with those in literature show some agreement. Sinibaldi et al. (1998) provided calculations of displacement speed for a downwardly propagating flame interacting with a toroidal vortex, and presented values of S_d/S_L in the range of 0 to 5.5. This compares to the values presented in this study of a maximum of 10. However, the results in this thesis show negative values of S_d/S_L which is not apparent in the work of Sinibaldi et al. (1998).

Figure 5 also presents the calculated local flame stretch rate with respect to distance around the flame surface for the flame/vortex interaction example. It is apparent from the data that large variations in local flame stretch rate correspond to variation in curvature as the flame surface is traversed. Again the initial measurement point corresponds to the lower right hand side of the flame front. As the data approaches the region of negative curvature where the flame front is curling over into the flow recirculation generated, a maximum peak in stretch rate of approximately 9000 s^{-1} occurs. The calculated stretch rate then varies in the region of the flame around the recirculation, before returning to an approximate constant along the upper uniform edge of the flame. In a similar manner to the data for normalised displacement speed, as the tip of the flame where interaction with the upper flow structures is apparent, variation in stretch rate is seen. At the points on the flame surface prior to and after the flame tip, where the surface demonstrates negative curvature, positive peaks in stretch rate can be seen of approximately 4500 s^{-1} and 3000 s^{-1}. Interestingly at the flame tip where the radius of curvature is small a minima in local stretch rate is calculated. Moving along the remainder of the flame surface, the stretch rate remains approximately constant until the segment of the flame interacting with the left hand side flow recirculation is approached. Here, as the curvature becomes negative, a positive peak in flame stretch rate occurs. Variations in stretch rate can again be seen in the region of negative curvature, before becoming approximately constant.

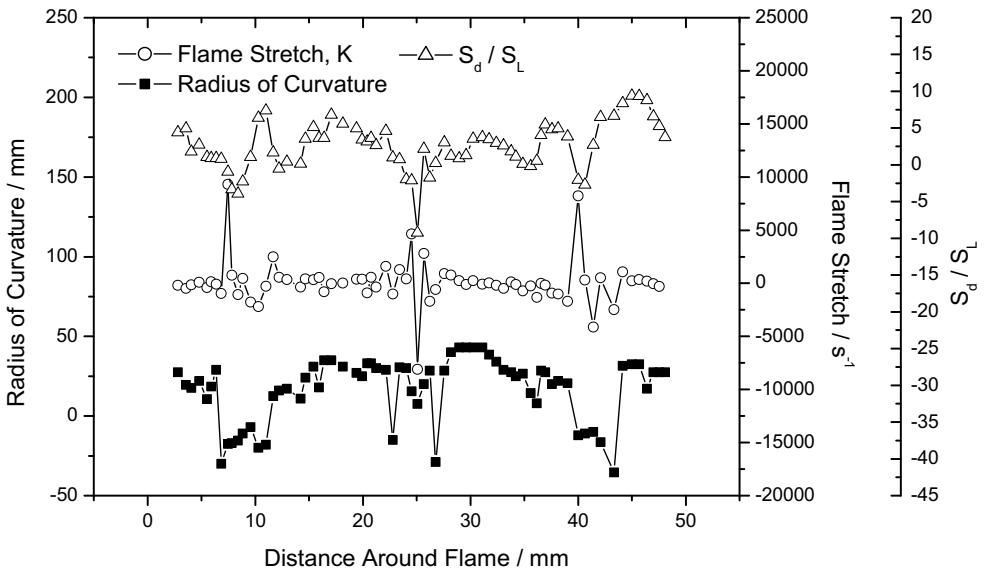

Fig. 5. Calculated variation with curvilinear distance around the flame front of radius of curvature, normalised flame displacement speed and flame stretch. Data obtained from the typical experimental run presented in Fig. 4.

A similar trend linking stretch rate and flame displacement speed can be seen in Fig. 5. Again moving from the lower right hand side of the flame front, peaks in the stretch rate can be tallied with negative values of flame displacement speed. Positive variations in S_d/S_L appear with approximately constant values of flame stretch rate. At the tip of the flame a minimum value of normalised displacement speed occurs, as discussed previously, which corresponds to a minimum in flame stretch rate of approximately –8000 s^{-1}. Symmetry in the results for flame curvature, and the presented flame displacement speed and stretch rate can be seen, with a repeat in the discussed trends along the left hand region of the flame surface.

4. Conclusion

The investigation of flame/vortex interactions utilising PIV techniques has provided characterisation of the turbulent flow structures generated, and the subsequent interaction with a propagating flame within a practical laboratory based environment. Characterisation of the vortex structures generated provided values in comparison to that within the flame-vortex regime diagram presented by Samaniego and Mantel (1999). The newly developed twin camera PIV diagnostic technique allowed the capture of flame and flow at two instances separated by 300 µs on the same experimental run. This provided data for both flame position and flow velocity during flame/vortex interactions. Analysis of the flame position and flow velocity data allowed calculation of local flame displacement speed, S_d. Positive values of S_d normalised by S_L for a typical flame-vortex interaction compared to previous findings of Sinibaldi et al. (1998) for a range of 0 to 5.5. Interestingly, negative values of S_d/S_L were also calculated, with a minimum of S_d/S_L = -10 found. Comparison of S_d/S_L with the radius of curvature of the flame front showed an apparent correlation, with variation in flame displacement speed. Calculation of the local tangential strain rate, and local flame stretch rate has been achieved. Results for local flame stretch rate show positive values upto 9000 s^{-1} and a minimum of –8000 s^{-1} for a typical flame/vortex interaction. Links between stretch rate, radius of curvature and displacement speed are apparent.

References

Borghi, R., in Recent Advances in Aerospace Science (Ed. Casci, C.), (1985), 117-138.
Eichenberger, D. A. and Roberts, W. L., Effect of Unsteady Stretch on Spark-Ignited Flame Kernal Survival, Combustion and Flame, 118 (1999), 469-478.
Ibarreta, A. F. and Driscoll, J. F., Measured Burning Velocities of Stretched Inwardly Propagating Premixed Flames, Proceedings of the Twenty-Eighth Combustion Symposium, (2000), 1783-1791, The Combustion Institute.
Lee, T. W., Lee, J. G., Nye, D. A. and Santavicca, D. A., Local Response and Surface Properties of Premixed Flames During Interactions with Karman Vortex Streets, Combustion and Flame, 94 (1993), 146-160.
Louch, D. S. and Bray, K. N. C., Vorticity in Unsteady Premixed Flames: Vortex Pair-Premixed Flame Interactions Under Imposed Body Forces and Various Degrees of Heat Release and Laminar Flame Thickness, Combustion and Flame 125 (2001), 1279-1309.
Mueller, C. J., Driscoll, J. F., Sutkus, D. J., Roberts, W. L., Drake, C. and Smooke, M. D., Effect of Unsteady Stretch Rate on OH Chemistry During a Flame-Vortex Interaction: to Assess Flamelet Models, Combustion and Flame 100 (1995), 323-331.
Mueller, C. J., Driscoll, J. F., Reuss, D. L. and Drake, C., Effects of Unsteady Stretch on the Strength of a Freely Propagating Flame Wrinkled by a Vortex, Proceedings of the Twenty-Sixth Combustion Symposium, (1996), 347-355, The Combustion Institute.
Mueller, C. J., Driscoll, J. F., Reuss, D. L., Drake, C. and Rosalik, M. E., Vorticity Generation and Attenuation as Vortices Convect Through a Premixed Flame, Combustion and Flame 112 (1998), 342-358.
Poinsot, T., Veynante, D. and Candel, S., Quenching Processes and Premixed Turbulent Combustion Diagrams, Journal of Fluid Mechanics, 228 (1991), 561-606.
Poinsot, T., Veynante, D. and Candel, S., Diagrams of Premixed Turbulent Combustion Based on Direct Simulation, Proceedings of the Twenty-Sixth Combustion Symposium, (1996), 612-619, The Combustion Institute.
Renou, B., Boukhalfa, A., Puechberty, D. and Trinité, M., Effects of Stretch on the Local Structures of Freely Propagating Premixed Low-Turbulent Flames with Various Lewis Numbers, The Proceedings of the Twenty-Seventh International Combustion Symposium, (1998), 841-847, The Combustion Institute.
Roberts, W. L. and Driscoll, J. F., A Laminar Vortex Interacting with a Premixed Flame Measured Formation of Pockets of Reactants, Combustion and Flame 87 (1991), 245-256.
Roberts, W. L., Driscoll, J. F., Drake, M. C. and Goss, L. P., Images of the Quenching of a Flame by a Vortex-To Quantify Regimes of Turbulent Combustion, Combustion and Flame 94 (1993), 58-69.
Samaniego, J. M. and Mantel, T., Fundamental Mechanisms in Premixed Turbulent Flame Propagation via Flame-Vortex Interactions Part I: Experiment, Combustion and Flame 118 (1999), 537-556.
Sinibaldi, J. O., Mueller, C. J. and Driscoll, J. F., Local Flame Propagation Speeds Along Wrinkled, Unsteady Stretched Premixed Flames, Proceedings of the Twenty-Seventh Combustion Symposium, (1998), 827-832, The Combustion Institute.

Author Profile

G. K. Hargrave: He received his Ph.D. in 1984 from the Department of Fuel and Energy, University of Leeds. His research work included studies of the structure and heat transfer from turbulent, premixed flames and the application of optical diagnostics for flow field characterisation in combustion systems. After his Ph.D. he worked in Research and Development for British Gas plc, where he specialised in the development and application of optical diagnostic techniques. His current position is a senior lecturer in Thermofluids in the Department of Mechanical Engineering at Loughborough University. His research interests include Particle Image velocimetry (PIV), Laser Induced Fluorescence (LIF) and High-Speed Imaging, with particular emphasis on their application to SI Engines, fuel injection systems, domestic and industrial burners, medical inhalers and the study of flame propagation in explosions.

S. Jarvis: He received his PhD. in 2003 from the Wolfson School of Mechanical and Manufacturing Engineering, Loughborough University. His research included the study of premixed flame interaction with turbulent structures using novel laser diagnostic techniques. After completing his PhD he worked at Loughborough University on research collaborations into soot formation within premixed burner flames. His current research at Loughborough involves the investigation of cycle to cycle variations within a optical single cylinder internal combustion engine, application of new PIV techniques, and fundamental flame propagation.